Characterization of AlSi and AlSi-$TiSi_2$ Metal-Semiconductor Contacts

Mark Davis, Advisor: Dr. Michael Jackson

ABSTRACT

The RIT SMFLs Flash Evaporator has a history of depositing a layer of aluminum with poor electrical and visual characteristics after sinter when deposited on Silicon, suspected to be due to the aluminum spiking into the substrate from a lack of Silicon. This project seeks to characterize this defect by examining the Aluminum films of the Flash Evaporation tool, Thermal Evaporation tool, and DC Sputter tool, both with and without a self-aligned $TiSi_2$ buffer layer. X-ray Photoelectron Spectroscopy (XPS) is used to determine the chemical composition of the layer, Transmission Line Measurements (TLMs) to determine contact resistivity, diodes to electrically detect spikes deeper than a specified threshold, and optical detection to characterize the frequency and geometry of the junction spikes as a function of contact area. A rough film defect was found to occur in every film, independent of deposition method, contact size, and the underlying layer. The defect in these devices was found to likely be Silicon hillocks nucleating above the substrates surface during the sinter, rather than the hypothesized junction spiking.

Keywords: Al, Junction Spiking, $TiSi_2$, XPS, TLM

1. INTRODUCTION

METAL interconnects are a necessity in nearly all semiconductor applications. Metal is the primary type of material for current transport with the lowest possible resistance. Resistance in metal interconnects comes in two forms, series resistance and contact resistance. Series resistance can be decreased by either choosing a material with the lowest bulk resistivity or increasing the cross sectional area that the current is passing through. Contact resistance is a function of the nature of the contact between a metal and a semiconductor. An ideal interconnect would have no series or contact resistance.

Aluminum has been used as a popular material for electrical interconnects in semiconductor manufacturing for decades. The availability of Aluminum paired with the relative ease of processing causes it to be a primary material to be used. Recently, 1% Aluminum-Silicon deposited with the Flash Evaporation system in RIT's SMFL have been affected by a defect, displayed in Figure 1.

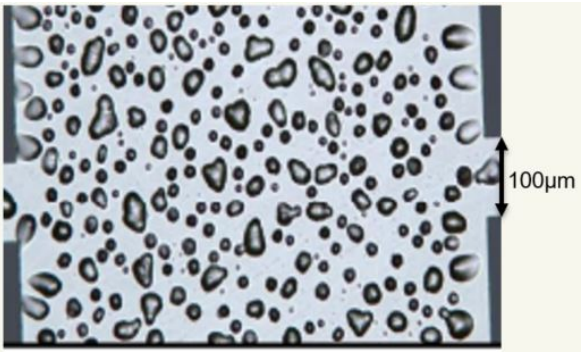

Figure 1. Sintered 1% AlSi Flash Evaporated Film Defect.[1]

This defect is hypothesized to be Aluminum junction spiking due to a lack of Silicon in the deposited film. Similarly, Aluminum-Silicon deposited with the DC Sputter system has been found to have a higher bulk resistivity than reported, hypothesized to be due to an excess of Silicon in the deposited film. This paper investigates the Metal-Semiconductor characteristics of 1% AlSi films deposited with the SMFL's Flash Evaporator, Thermal Evaporator, and CVC 601 DC Sputter systems. Additionally, a $TiSi_2$ buffer film is included to prevent junction spiking, as well as characterize contact resistance.

2. THEORY

2.1 Aluminum Junction Spiking

Aluminum Films on Silicon substrates are typically sintered at approximately 450°C. This sintering step has many benefits to the electrical characteristics of the film, such as ensuring any metal-semiconductor contact is ohmic rather than rectifying. At 450°C, Aluminum and Silicon have a relationship shown in Figure 2.

Mark Davis is a student at Rochester Institute of Technology in the Department of Electrical and Microelectronic Engineering.

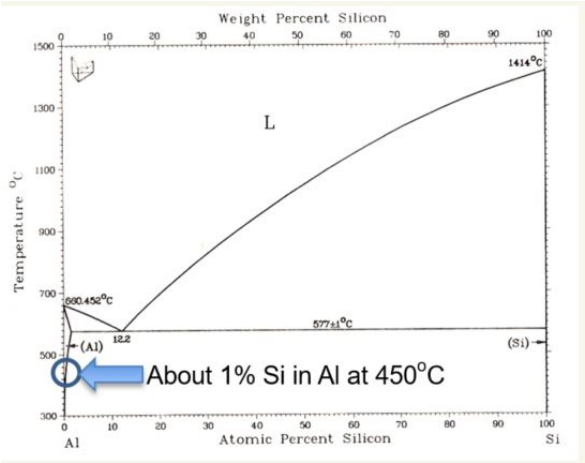

Figure 2. Aluminum-Silicon Phase Diagram.[2]

At 450°C, there is approximately 1% Silicon by weight within the Aluminum. When a Silicon starved film is at this temperature, the film will seek out this 1% Silicon. Typically, the Silicon comes from the substrate. This causes pits or spikes to form in the substrate, which are locations where the silicon migrated into the film leaving the spike for the Aluminum to conform to.[3] This is illustrated in Figure 3.

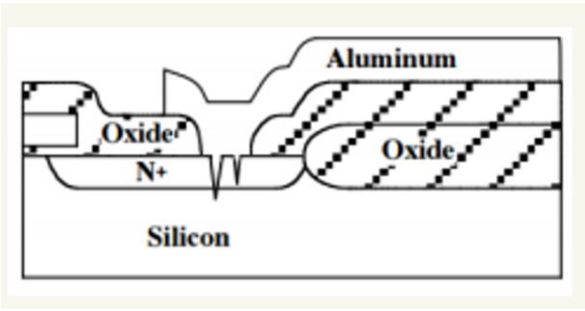

Figure 3. Cross Section of Junction Spiking.[4]

The danger of this defect is if there is a junction that is more shallow than the spike depth, the Aluminum within the spike will electrically connect the junction, shorting the device. This usually causes total device failure, and is therefore a very significant defect to avoid.[3] At 450°C, Silicon can diffuse into Aluminum approximately 100 μm in 30 minutes (the standard sinter conditions),[4] which is more than enough to spike through electrical junctions.

2.2 X-Ray Photoelectron Spectroscopy (XPS)

XPS is an analysis that takes advantage of a photon's ability to transfer energy to a bound electron, ejecting it from a solid. Within an XPS system, there is an X-ray source that focuses onto the surface of a solid material, which transfers energy to an electron. This Photoelectron emits from the solid and is filtered and counted by kinetic energy. The collected data is compiled and organized as a function of "Binding Energy", with the output typically being counts per second (cps). The binding energy of practically every material within many matrices (chemical compositions) are known discrete values, meaning that with no prior knowledge of what an analyzed material is, the sample can be identified with XPS to about a 0.5%[5] accuracy. An Image of the basic operation of an XPS test is given in Figure 4.[3]

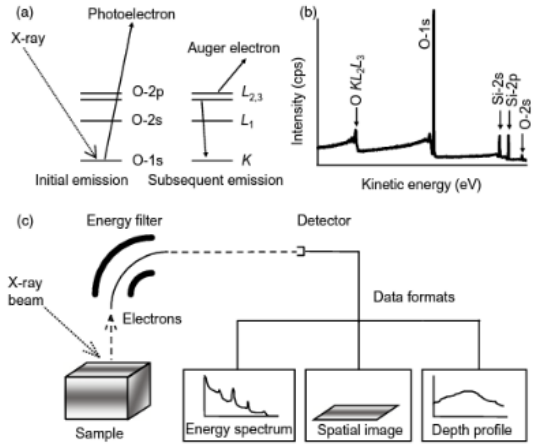

Figure 4. XPS Operation.[5]

2.3 Transmission Line Measurements (TLMs)

TLMs are a series of resistors are varying and known distances apart, shown in Figure 5.

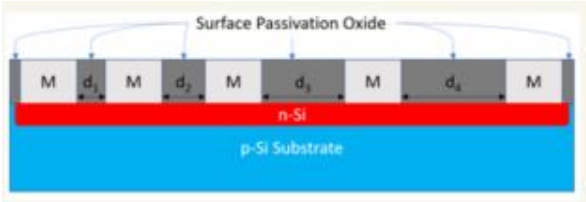

Figure 5. TLM Cross Section.

A TLM is used for extrapolating contact resistance (ρ_c) and transfer length (L_T). Contact resistance is the electrical resistance of the current transferring from the semiconductor to the metal contact. Transfer length is the average distance that the carriers travel before travelling into the contact. A graph showing a TLM's ideal electrical characteristics is given in Figure 6.

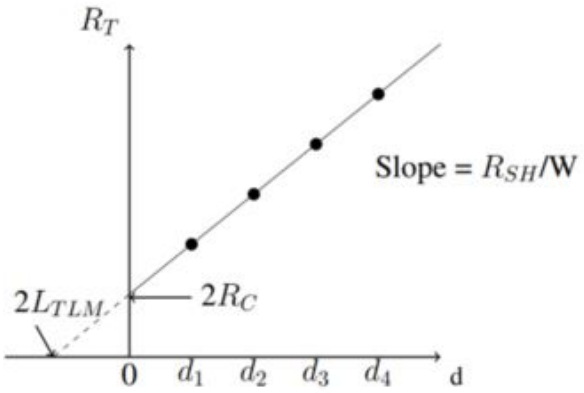

Figure 6. TLM Electrical Characteristics.[4]

In this study, the goal is to find a relative ρ_c as a function of Silicon percentage, transfer length isn't considered.

2.4 Diodes

The purpose of the diodes in this study is to electrically detect a junction spike, in the form of a short circuit. As previously mentioned, Silicon can diffuse 100 μm into Aluminum, and therefore a diode with a junction shallow enough can detect spiking past a certain threshold. The expected effect of a junction spike shorting these diodes is shown in Figure 7.

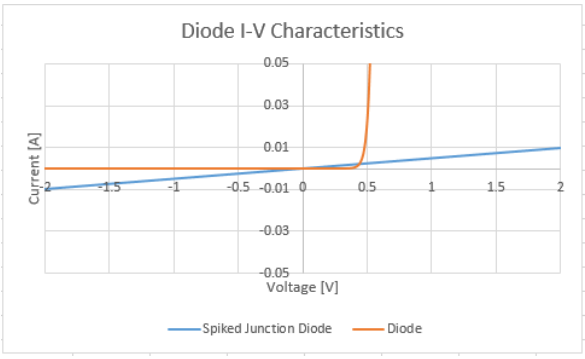

Figure 7. Spiking Diode Electrical Characteristics.

2.5 Visual Analysis

The Diodes used to detect junction spiking are also used to examine the surface of the Aluminum film for optical defects similar to Figure 1. The diode contacts, after the 450°C sinter, are examined in a microscope and pictures of them taken. Using the ImageJ image manipulation/analysis software, the defect density (number of defects per unit area) and average defect size can be characterized. The diodes have varying contact areas from 100 μm to 10,000 μm, to examine the defect density and size as a function of contact area. The ImageJ analysis methodology is provided in Figure 8.

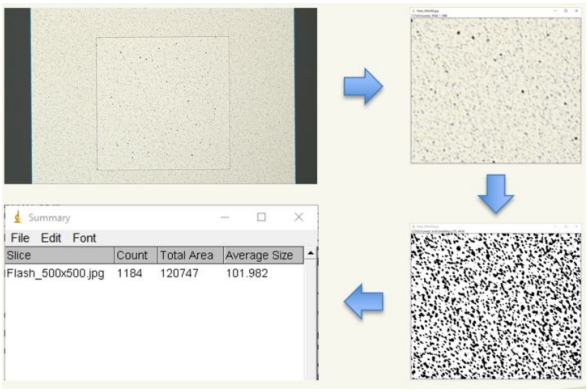

Figure 8. Image Analysis in ImageJ.

The analyzed images were all taken under the same magnification conditions and with the same resolution, therefore in ImageJ a global scale can be set, converting the dimensions from pixels to μm. The images appear to be uniformly illuminated, but there is a lighting gradient that creates significant noise in the defect analysis. To correct for this, the images are cropped to local regions of the image, where the lighting is much more uniform. The image is then converted to 16-bit gray scale, which is necessary in order to use the threshold tool. The image is thresholded, converting the image to a binary map where particles are black and the unaffected area of the film is white. In this format, a particle analysis can be run which counts the number of black defect as well as the size of each defect.

3. FABRICATION

3.1 XPS Samples

The samples to be used for XPS analysis were deposited onto glass substrates. Slides were prepared with a brief Acetone and Isopropal Alcohol rinse, followed by Aluminum deposition via Sputter and Flash Evaporation. The Thermal Evaporation sample used was the 1% AlSi pellet Flash Evaporation source.

3.2 Device Wafers

The device fabrication general process flow is shown below in Figure 9.

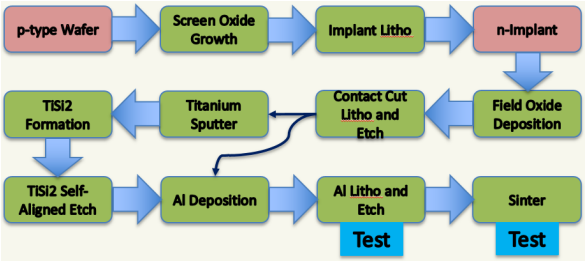

Figure 9. General Process Flow.

Fabrication began with a 10 Ω-cm p-type (100) Cz Silicon wafer. This was selected for compatibility with previous processes, but led to problems discussed later in this section. A 500$\AA$ screen oxide was grown as an implant buffer layer, and an implant define photoresist was patterned. The wafers were then shipped externally for a P31 n-type implant with a dose of 4E12 cm^{-2}, which contributed to electrical issues discussed below. After electrical activation via a furnace well-drive, a surface passivation SiO_2 layer was deposited with PECVD, and contacts regions were etched. At this stage, the devices were allocated with or without $TiSi_2$. The devices with the intermediate layer were sputtered with Titanium, followed by an anneal step forming TiSi. A self aligned etch in Piranha (H_2SO_4 and H_2O_2) removed the unreacted Titanium, leaving the Silicide in the contact region. Following another anneal to form $TiSi_2$, Aluminum was deposited and patterned on every wafer via Flash Evaporation, DC Sputter, or Thermal Evaporation. The devices were then electrically tested, sintered at 450°C for 30 minutes, and tested again.

The p-type substrate choice compounded with the low dose n-type implant to cause major electrical issues. Aluminum is a p-type metal, and therefore will theoretically rectify (creating a Schottky diode-like characteristic) with the n-type contact regions of the TLMs and diodes. The very low dose implant caused thermionic emission rather than field emission of the carriers from the semiconductor to the metal, creating more rectification effects. A more optimal process flow would begin with an n-type wafer and have a high dose (1E15 cm^{-2} or higher) B11 p-type implant, creating ideal M-S contacts to extract contact resistance data.

4. RESULTS AND DISCUSSION

4.1 XPS

The XPS analysis was carried out with the aid of a Focused Ion Beam (FIB). The FIB was used to "dig" into the samples, analyzing the bulk of the film rather than the contaminated surface. The spectra of the three samples, after the analysis reached the bulk regime of the samples, is given in Figure 10.

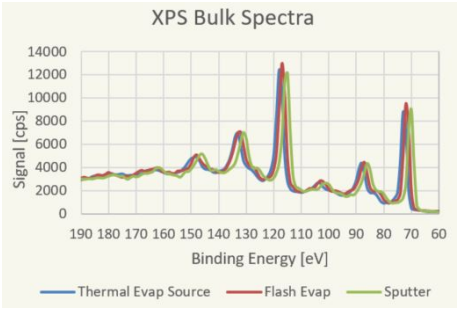

Figure 10. XPS Spectra of AlSi Samples.

These samples have a slight offset because these spectra are pre-calibration, but once the energy calibration is carried out the x-alignment of the peaks is perfect. An issue with the XPS results is the signal of the Aluminum peaks includes Plasmon peaks, which are energy loss features from the primary peaks. The second Plasmon peak of Aluminum's 2p peak directly corresponds with Silicon's peaks. This phenomenon is displayed in Figure 11.

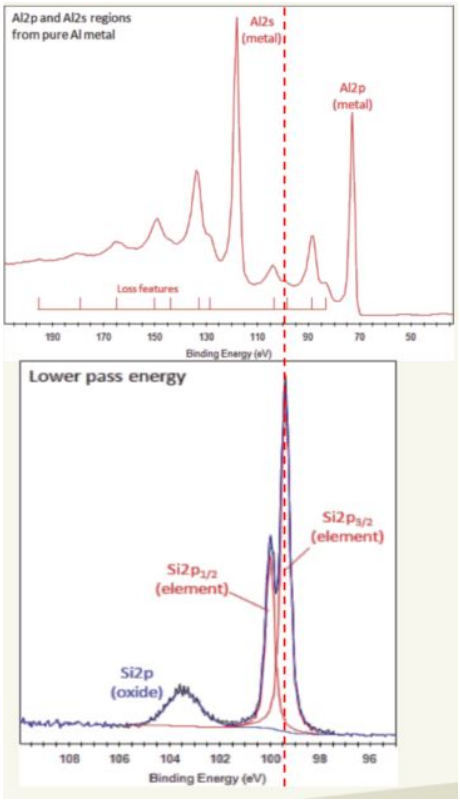

Figure 11. Characteristic XPS Spectra of Al and Si.[6]

This overlap wouldn't be as much of an issue if the

samples had a high concentration of Silicon, as the deconvolution would be fairly trivial. Unfortunately, the expected Si content of 0.5-1.5% in the samples caused the Si peaks to fall largely within the noise margin of the Al Plasmon peak. The peaks were deconvolved to obtain percentage values, but the validity of these values is questionable. The extracted data is given in Figure 12, with percentage of Silicon being plotted against FIB sputter time.

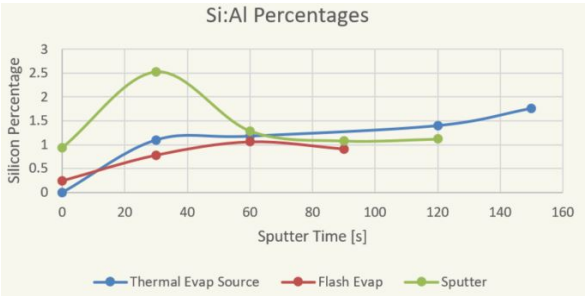

Figure 12. Si Percentage vs FIB Sputter Time.

In this figure, the FIB sputter time conveys an arbitrary depth, not necessarily uniform between the samples at corresponding times. The bulk percentages were extracted for relative analysis by examining when the signal reached a pseudo-steady state, and averaging those values. Through this method, the results in Table 1 were extracted. The expected results were a Silicon starved Flash Evaporated film, Silicon rich Sputtered film, and on-target Thermal Evaporated film. While the Flash Evaporated sample did have less Si than the Thermal, the Sputtered film had even less.

Sample	Bulk %	Normalized Amount
Thermal Evap	1.29	1
Flash Evap	0.916	0.71
Sputter	1.1	0.85

Table 1. Normalized Bulk Si Percentages

4.2 TLM Analysis

As mentioned in the Theory section, the TLMs were not expected to function well electrically. A general resistor measurement for each sample is shown in Figure 13.

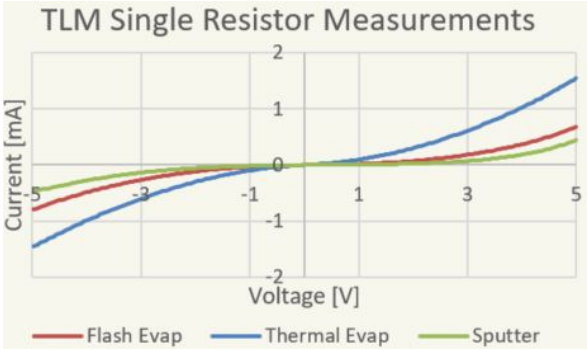

Figure 13. Rectifying TLM Resistor.

These I-V characteristics display contacts rectifying in both polarities, with a large amount of series resistance. Extracting resistance was attempted for relative analysis, but unfortunately the results were not indicative of valid TLM analysis. An example of the TLM data is given in Figure 14.

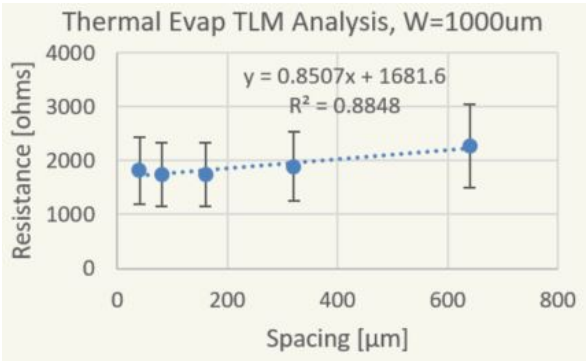

Figure 14. TLM Graph.

While this graph does have the correct general TLM trend with a fair R^2 value, the error margin of over 30% invalidates any trend, as a trend in the opposite direction is also within that margin. This is indicative of the fact that many of the individually tested TLMs had a reverse trend of the resistance going down as contact spacing decreases. Overall, the TLMs on every wafer showed the rectifying behavior, and contact resistance could not be extracted, both before and after sinter.

4.3 Diode Analysis

The diode electrical analysis yielded varying results for each sample. Before sinter and after sinter results are shown in Figures 15-17.

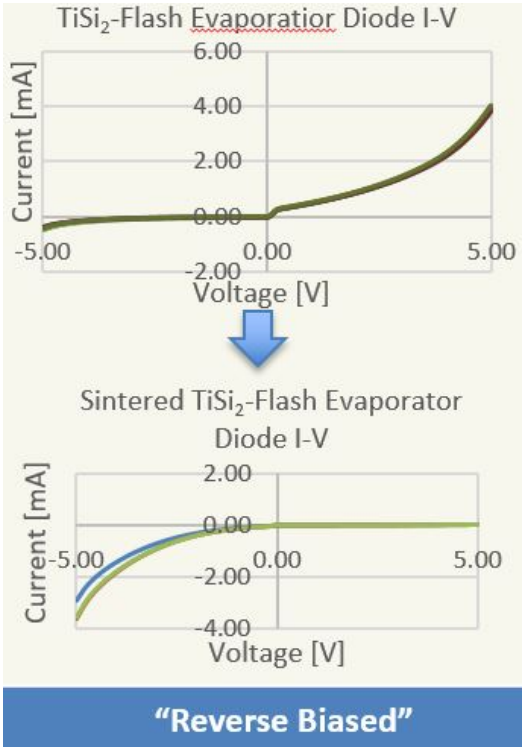

Figure 15. Sinter's Effect on $TiSi_2$-Flash Evap Diodes.

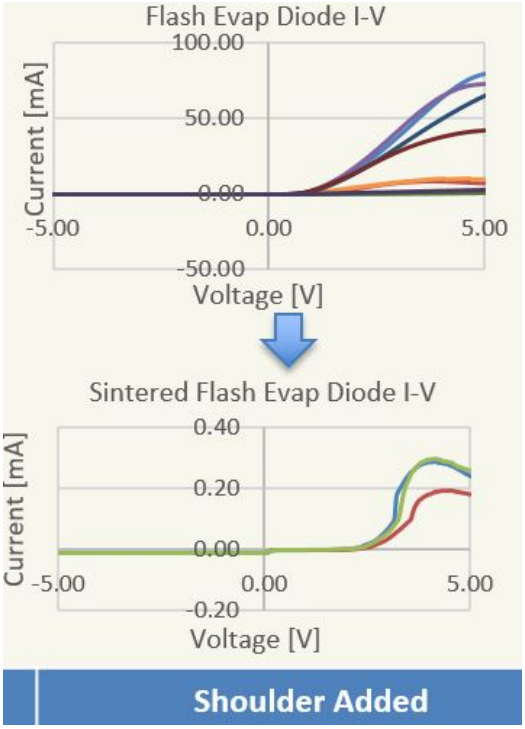

Figure 16. Sinter's Effect on Flash Evap Diodes.

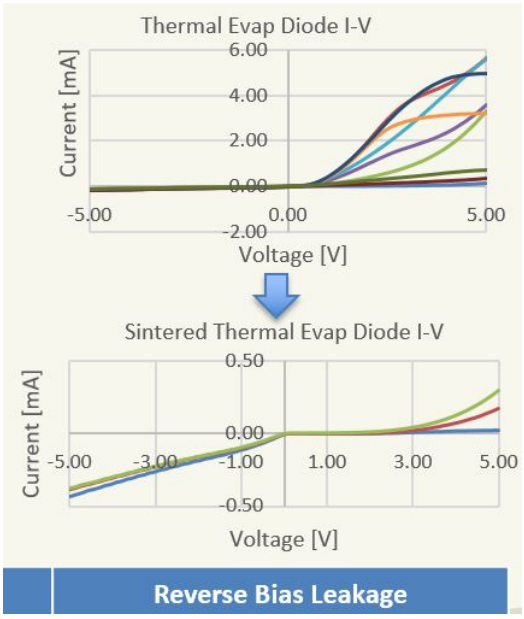

Figure 17. Sinter's Effect on Thermal Evap Diodes.

The $TiSi_2$ buffered diodes all exhibited a behavior in which they appeared to opperate similar to a reverse biased diode. This is interesting because the sinter at 450°C shouldn't affect the $TiSi_2$ layer, which is formed at 800°C.
The diodes on the Flash Evaporator sample exhibited a shoulder after sinter, which looks similar to the beginning of an Esaki tunnel diode.
The diodes on the Thermal Evaporator sample had a liner reverse bias leakage after sinter.
These effects were unexpected, as the only anticipated change would have been a short from junction spiking, shown in Figure 7.

4.4 Visual Analysis

A cross section of the imaged regions is shown in Figure 18.

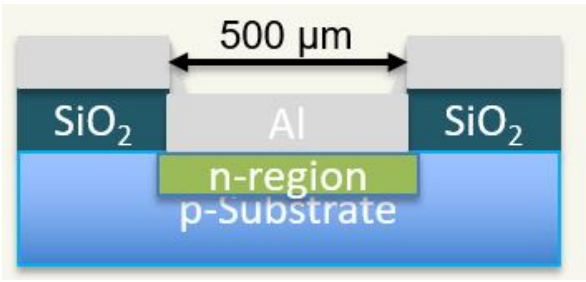

Figure 18. Visual Area Cross Section.

4.4.1 Optical Microscopy

Before the devices were sintered, the film appeared relatively defect-free. The images of each film post-sinter are shown below in Figure 19.

Figure 19. 10x Microscope Images of Sintered Films.

It was expected that a visual defect would only appear in the Flash Evaporated film, where the Aluminum is touching the Silicon without a buffer. After sinter, every film exhibited visual defects throughout. The films were analyzed as outlined in the Theory section, leading to Figures 20-21.

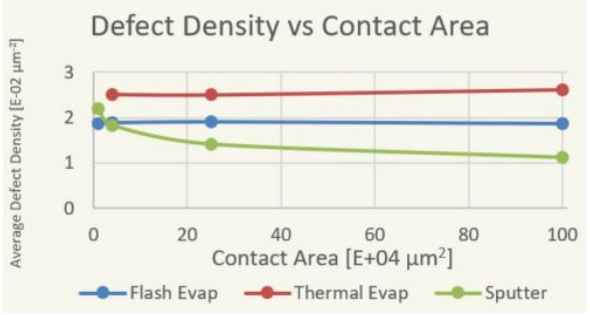

Figure 20. Defect Density vs Contact Area.

Figure 21. Defect Size vs Contact Area.

Both of these graphs display that there isn't a specific dependence of defect density and size on contact area. There seems to be a trend in which the Sputtered film has the lowest Defect Density and the largest defect size, but that is believed to be due to a de-focus of the microscope's objective lens, causing particles to bunch together forming seemingly larger particles. The defect density and size as a function of the XPS measured Silicon percentage are given in Figures 22 and 23.

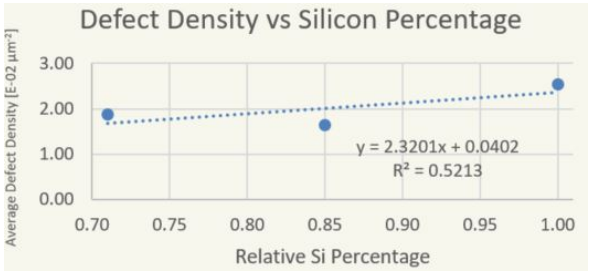

Figure 22. Defect Density vs Relative Si Percentage.

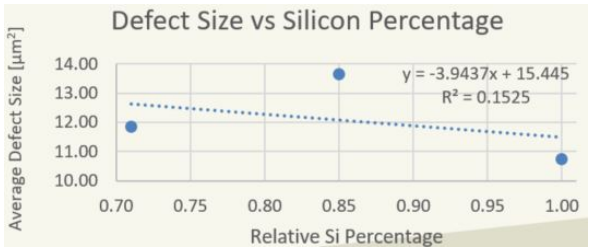

Figure 23. Defect Size vs Relative Si Percentage.

Both of these graphs revealed that neither the defect density nor the defect size were a function of the measured Si percentage, as R^2 values of 0.5 and 0.15 are far too low.

4.4.2 Scanning Electron Micrographs (SEM)

The Aluminum was stripped from the Silicon via wet etch, and the defects remained visible on the optical microscope on every sample, directly corresponding to

the defects visible in the Aluminum film To investigate this, a piece from the Flash Evaporator sample was examined with an SEM. The resultant images are shown in Figure 24.

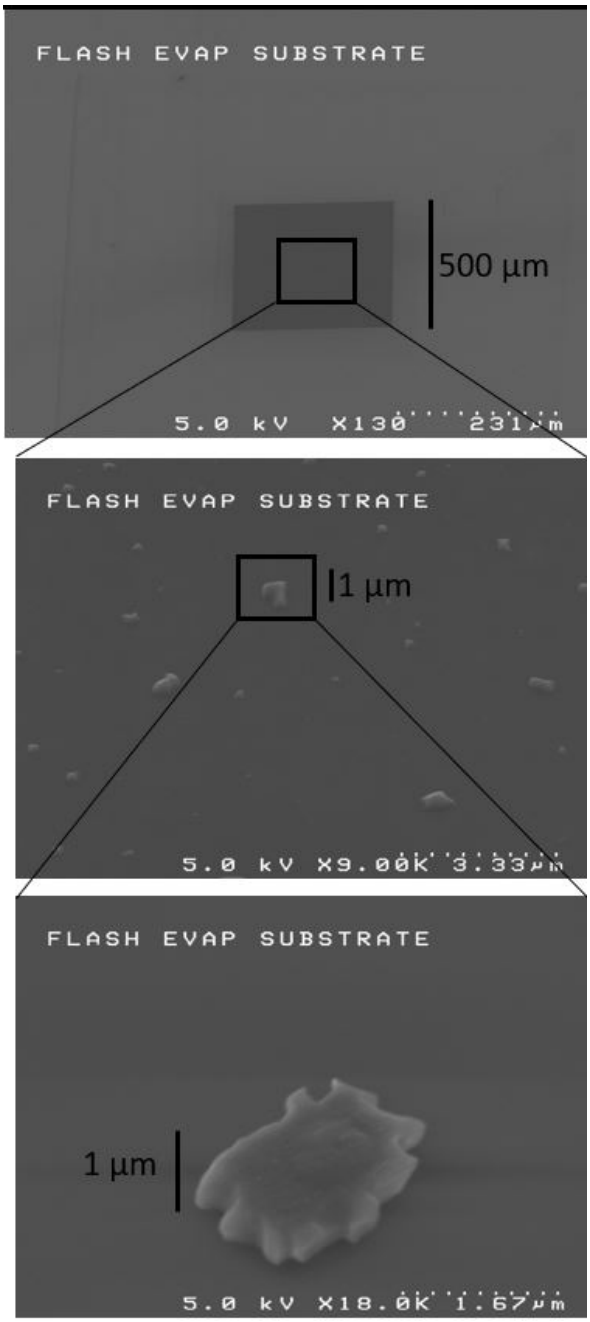

Figure 24. SEM Images of Defects on Flash Evap Substrate.

It was hypothesized that the defect was junction spiking, which would result in pits formed in the Silicon after the sinter. After the film is stripped, the SEM images would display those pits. Instead, Figure 24 shows the defect to be particles on the substrate roughly 1800 $\mathring{A}$ tall, meaning the defect within this study is likely not junction spiking.

5. CONCLUSION

Due to the findings from the SEM and the optical microscope images, the defect found within the three deposited films is not junction spiking. The particles are likely Silicon hillocks that nucleated during the sinter. The hillocks appear to be similar to the defect reported in Figure 1, but is not necessarily the same defect.

5.1 Future Work

Further studies of this defect include ordering Auger or SIMS analysis of the Aluminum films to more accurately measure the Silicon percentages, the process modifications discussed in the Fabrication section, and EDS analysis of the post-sinter etched films to determine the chemical makeup of the particles.

6. ACKNOWLEDGMENTS

I would like to thank my project advisor Dr. Jackson for the project inspiration, as well as Dr. Dale Ewbank and Dr. Robert Pearson for the guidance throughout the project, and Dr. Lynn Fuller for his seemingly endless processing knowledge. This project wouldn't be where it is without the immense help of many of my peers, specifically Matt Hartensveld for SEM imaging. Lastly, I'd like to thank the SMFL staff for the continuous support in the clean room.

REFERENCES

1. K. S. Duggimpudi, "Characterization of grid contacts for n-si emitter solar cells," Master's thesis, Rochester Institute of Technology, 2016.
2. M. Shamsuzzoha, *Aluminium Alloys for Transportation, Packaging, Aerospace, and Other Applications*, 2007.
3. M. Davis, *Measurement of Silicon Concentration in Flash Evaporated and Sputtered Aluminum with ESCA*. Metrology, 2016.
4. S. Grover, "Effect of transmission line measurement (tlm) geometry on specific contact resistivity determination," Master's thesis, Rochester Institute of Technology, 2016.
5. P. van der Heide, *X-ray Photoelectron Spectroscopy*, 1st ed. Wiley, 11 2011.
6. T. Scientific. (2018) Xps simplified. [Online]. Available: https://xpssimplified.com/periodictable.php